A Comparative Study of the Energy-Saving Controllers for Automotive Air-Conditioning/ Refrigeration Systems

Yanjun Huang[1]
Department of Mechanical and Mechatronics Engineering,
University of Waterloo,
Waterloo, ON N2L3G1, Canada
e-mail: y269huan@uwaterloo.ca

Amir Khajepour
Department of Mechanical and Mechatronics Engineering,
University of Waterloo,
Waterloo, ON N2L3G1, Canada
e-mail: a.khajepour@uwaterloo.ca

Milad Khazraee
Department of Mechanical and Mechatronics Engineering,
University of Waterloo,
Waterloo, ON N2L3G1, Canada
e-mail: milad.khazraee@uwaterloo.ca

Majid Bahrami
School of Mechatronic System Engineering,
Simon Fraser University,
Surry, BC V3T 0A3, Canada
e-mail: mbahrami@sfu.ca

With the extensive application of air-conditioning/refrigeration (A/C-R) systems in homes, industry, and vehicles, many efforts have been put toward the controller development for A/C-R systems. Therefore, this paper proposes an energy-saving model predictive controller (MPC) via a comparative study of several control approaches that could be applied in automotive A/C-R systems. The on/off controller is first presented and used as a basis to compare with others. The conventional proportional-integral (PI) as well as a set-point controller follows. In the set-point controller, the sliding mode control (SMC) strategies are also employed. Then, the MPC is elaborated upon. Finally, the simulation and experimental results under the same scenario are compared to demonstrate how the advanced MPC can bring more benefits in terms of performance and energy saving (10%) over the conventional controllers.
[DOI: 10.1115/1.4034505]

Keywords: air-conditioning/refrigeration system, energy-saving sliding mode control, model predictive control

1 Introduction

Considerable amounts of energy are being consumed as A/C-R systems have been extensively adopted in residences, industry, as well as vehicles [1]. Meanwhile, researchers are driven to design more efficient and green devices because of the continuously increasing demands on energy conservation and environment protection. It is known that efficient operation of A/C-R systems could bring significant benefits in terms of operating costs and effects on the environment [2]. For any A/C-R system, an important step in making it work efficiently is to apply a proper control strategy. Therefore, this paper will focus on presenting the controller development process as well as the simulation, validation, and comparison work. The comparison results show that the MPC as the promising controller can not only save about 10% energy but also enhance the controlled temperature performance under the examined condition.

A literature review on the existing controllers of A/C-R systems is presented in Sec. 2 followed by the difference discussion; then, a simplified model based on moving boundary and lumped parameter method is briefly introduced. Several controllers from the conventional to the advanced are developed step by step in Sec. 6. In addition, the simulation and experimental results of the controllers are presented and compared to demonstrate the advantages of the advanced MPC. In Sec. 7, comments and future work are discussed.

2 Previous Research

In general, the compressor, the evaporator, the expansion valve, and the condenser—the four main components connecting end to end—form the vapor compression cycle or A/C-R system, as presented in Fig. 1. Due to extensive applications of A/C-R systems in different fields, many researches with different objectives have been conducted on their controller development, which could be summarized as: (1) proper temperature or humidity of a specific area; (2) improvement of system steady-state performance and robustness; and (3) reduction of energy consumption [3].

The on/off controller was initially introduced because of its simplicity and ease of application. It is capable of maintaining the controlled temperature within a certain range by turning the compressor on or off. However, it is unable to schedule the temperature oscillation amplitudes when conditions are changing, such as the ambient temperature and varying temperature requirements. In addition, frequent compressor on/off activations can lead to excessive power consumption and cause mechanical components to wear over time [3]. More importantly, energy saving is not of any importance in on/off controllers, which is the reason why Leva et al. [4] and Li et al. [5] improved the original on/off controller by adding adaptive or optimization algorithms to make it more efficient. Nevertheless, the nature of such a controller hinders its enhancement to a large extent. In recent years, the employment of continuous variable components in the A/C-R system makes the development of more efficient controllers possible. Especially, as the anti-idling technologies and electric vehicles become more and more popular, the electrification technology of the A/C-R

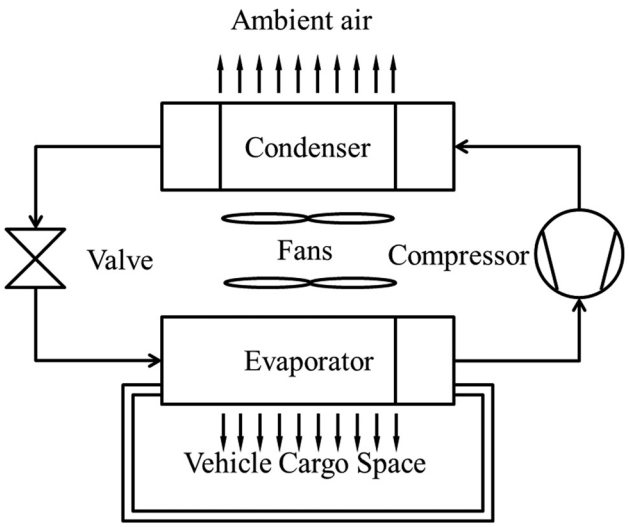

Fig. 1 Schematic diagram of an A/C-R system

[1]Corresponding author.
Contributed by the Dynamic Systems Division of ASME for publication in the Journal of Dynamic Systems, Measurement, and Control. Manuscript received November 10, 2015; final manuscript received August 10, 2016; published online October 17, 2016. Assoc. Editor: Yang Shi.

system in the vehicle will separate the compressor from the engine such that the compressor is able to actively change its speed instead of passively following the engine speed. The current controllers of A/C-R systems other than the on/off one can be classified into three types: the classic feedback controller, the intelligent controller, and the advanced controller [4] or the classical control, the soft controller, and the hard controller [6]. As the most popular type of conventional feedback controller, the PI controller has been used for a long period. A relevant example is the superheat-expansion valve and temperature-compressor control [7]. This continuous feedback controller could indeed reduce mechanical wear of the compressor. However, it is hard to tune the controller parameters due to the nonlinear and multi-input multi-output nature of A/C-R systems. Petersen and Lund in Ref. [8] proposed a method to decouple the controllers. This conventional feedback control strategy considers system efficiency by controlling superheat in the evaporator [9].

Artificial intelligent control techniques including artificial neural network (ANN) control, fuzzy logic control, expert system, etc., have been utilized to treat nonlinearities or uncertainties in A/C-R operation processes. In some cases, these control approaches are combined with A/C-R system control [4]. However, Ref. [10] mentions their limitations, which include over training, extrapolation, network optimization, and their not being optimal, all of which impede their development.

Koo et al. [11] presented a second-order SMC for the single-input single-output refrigeration system, which regulates the superheat by manipulating the compressor speed. This controller can also effectively alleviate chattering phenomenon but does not directly deal with power consumption. Shah et al. [12] presented a multivariable adaptive controller. The idea behind is that this controller is able to identify different linear models for a nonlinear system over the domain of operating conditions, so it is a kind of nonlinearity compensation for a general dynamic system. There are other kinds of nonlinearity compensation controls like robust control and gain scheduling control [13,14]. Larsen proposed two kinds of optimization control methods [15]: set-point optimizing control and dynamic optimizing control. In all of these advanced control methods, the MPC is a most successful and promising control algorithm, which can simultaneously deal with more than one objective to achieve multi-objective control such as the temperature, humidity, energy saving, enhancement of air quality, and improvement of steady-state performance and robustness [16–23]. Furthermore, it is very powerful when future related information is known as a priori [16] and used in constrained systems [17,18]. A comprehensive review of the controllers, especially the MPCs, for the Heating ventilation air conditioning systems in buildings was reported in Refs. [6] and [19]. Authors in Ref. [20] developed an adaptive MPC for a reefer container by combining a linearizing controller and a MPC, which ran once per hour due to the large computational efforts and included some constraints as barriers in the objective function instead of taking the advantage of MPC strategy for constraint treatment. In Ref. [21], an online trained ANN was utilized as the model to design a MPC for temperature manipulation without concern for energy saving, and it needed extra efforts for the online training.

3 Differences From the Previous Work

For all of these MPC algorithms developed for A/C-R systems in the existing literatures, energy consumption as a part of the objective function has seldom been considered, and computational cost is a serious issue since a MPC usually involves a complex online optimization to decide the optimal control law [3]. Recently, several solutions have been proposed such as the offline optimization [22], a combination of a branch-and-bound search technique to alleviate the computational cost of iterative optimization techniques [23]. Due to the existing problems, this paper proposes a linear discrete MPC for an automotive A/C-R system with three discrete compressor speeds. The proposed linear MPC can shorten the computation time and be implemented into real systems. First, a simplified control-oriented dynamic model of the A/C-R system is developed, which is improved from the one presented in Ref. [24] and can capture the dominant dynamics of the A/C-R system while keeping the simplicity compared to the data-driven model such as ANN type model. Second, a linear discrete MPC is designed based on the proposed model to regulate the temperature of the cargo space and minimize the energy consumption. Thanks to the simplicity of the model, the linear MPC only takes tens of milliseconds compared to several seconds or even minutes for the online optimization process for A/C-R systems in current literatures. The simulation and experimental results show the ability of the proposed MPC to immediately react to the large disturbances. It is also possible to run several optimization processes simultaneously in one time instant for the discrete MPC development. In addition, a series of control techniques are implemented, simulated, and experimentally tested to demonstrate the advantages of the proposed discrete MPC. Furthermore, the whole design process can be extended to the A/C-R systems with fully variable varying components. Due to the fact that there is no minimum constraint (other than zero) on the compressor speed of those systems, and the compressors are able to operate at a lower-speed to meet the requirement while pursuing the minimum energy consumption. In this scenario, the continuous MPC can help the system save more than 20% energy. Above all, this discrete MPC can not only achieve the temperature control objective in presence of the ambient disturbance but also realize about 10% energy saving compared to the conventional controllers under the same examined condition.

4 Modeling

The simplified dynamic model of the A/C-R system and cargo space are provided and comprehensively validated in Ref. [25]. In this paper, only the main dynamic equations are provided and briefly explained.

4.1 Expansion Valve. The expansion valve is assumed to be isenthalpic, i.e., the enthalpy at the inlet of the valve is identical to that at the outlet. No matter what kind of expansion valve it is, the refrigerant mass flow rate $(\dot{m}_v)$ through the expansion valve is modeled by

$$\dot{m}_v = C_v A_v \sqrt{\rho_v (P_c - P_e)} \tag{1}$$

For different types, the discharge coefficient (C_v) and the valve opening area A_v have different correlations obtained by experimental data [26–29].

4.2 Compressor. The dynamics of the compressor can be demonstrated by

$$\dot{m}_{\text{comp}} = N_{\text{comp}} V_d \eta_{\text{vol}} \rho_{\text{ref}}(P_e) \tag{2}$$

$$h_{\text{oc}} = \eta_a (h_{\text{is}}(P_e, P_c) - h_{\text{ic}}(P_e)) + h_{\text{ic}}(P_e) \tag{3}$$

Equation (2) depicts the refrigerant mass flow rate throughout the compressor with respect to compressor speed, and Eq. (3) shows the enthalpy change of refrigerant after going through the compressor [24].

4.3 Fin-Tube Type Evaporator. Two common types of heat exchangers are used in A/C-R systems: fin-tube type and microchannel type. The modeling method proposed in Ref. [3] is suitable for both types. More importantly, the modeling method takes the fins' effects into consideration and lumps it into two parameters such that the model is simple and accurate.

The three-state evaporator model can be written as

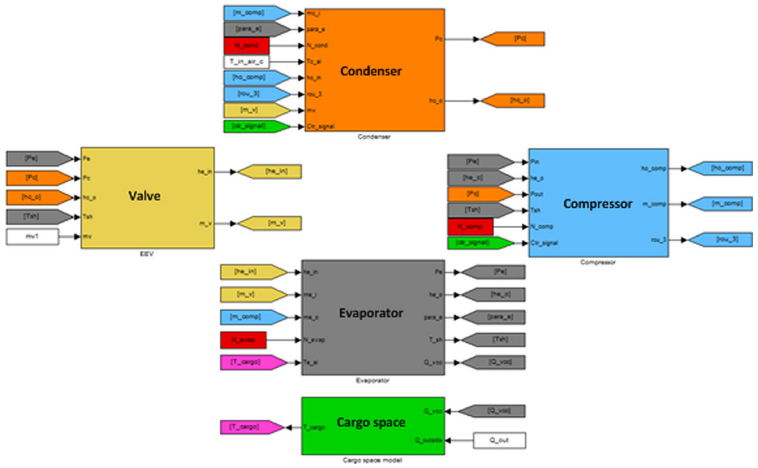

Fig. 2 Simulink model

$$h_{\mathrm{lge}}\rho_{\mathrm{le}}(1-\bar{\gamma}_e)A_e\frac{dl_e}{dt}=\dot{m}_v(h_{\mathrm{ge}}-h_{\mathrm{ie}})-\alpha_{\mathrm{ie}}\pi D_{\mathrm{ie}}l_e(T_{\mathrm{wfe}}-T_{\mathrm{re}}) \quad (4)$$

$$A_eL_e\frac{d\rho_{\mathrm{ge}}}{dP_e}\frac{dP_e}{dt}=\dot{m}_v\frac{h_{\mathrm{ie}}-h_{\mathrm{le}}}{h_{\mathrm{lge}}}-\dot{m}_{\mathrm{comp}}+\frac{\alpha_{\mathrm{ie}}\pi D_{\mathrm{ie}}l_e(T_{\mathrm{wfe}}-T_{\mathrm{re}})}{h_{\mathrm{lge}}} \quad (5)$$

$$(C_pm)_{\mathrm{wfe}}\frac{dT_{\mathrm{wfe}}}{dt}=\alpha_{\mathrm{oe}}A_{\mathrm{oe}}(T_{\mathrm{ae}}-T_{\mathrm{wfe}})-\alpha_{\mathrm{ie}}\pi D_{\mathrm{ie}}l_e(T_{\mathrm{wfe}}-T_{\mathrm{re}})-\alpha_{\mathrm{iesh}}\pi D_{\mathrm{ie}}(L_e-l_e)(T_{\mathrm{wfe}}-T_{\mathrm{re}}) \quad (6)$$

where the three states refer to length (l_e) of the two-phase section, pressure (P_e) of the evaporator, and equivalent temperature (T_{wfe}) of tube wall and fins. Equation (4) simulates the energy transfer from the refrigerant to the heat exchanger tube wall and fins of the two-phase section [14]. Equation (5) denotes the vapor refrigerant change rate throughout the evaporator tube. The first term on the right-hand side of this equation is the vapor mass at the inlet of the evaporator. Equation (6) reflects the heat conduction of the whole heat transfer process. The air-side heat transfer coefficient α_{oe} is changing with the speed of evaporator fan (N_{evap}).

4.4 Microchannel Type Condenser. Obviously, the total mass (m_{total}) of the refrigerant inside the cycle is constant without considering the leakage. The mass of refrigerant outside of the two heat exchangers is defined as (m_{pipe}). Thus, the difference between these two masses is the mass inside the evaporator and condenser, which can be shown by

$$m_{\mathrm{total}}-m_{\mathrm{pipe}}=A_e[\rho_{\mathrm{le}}l_e(1-\bar{\gamma}_e)+\rho_{\mathrm{ge}}l_e\bar{\gamma}_e+\rho_{\mathrm{she}}(L_e-l_e)]+A_c[\rho_{\mathrm{lc}}l_c(1-\bar{\gamma}_c)+\rho_{\mathrm{gc}}l_c\bar{\gamma}_c+\rho_{\mathrm{shc}}(L_c-l_c)] \quad (7)$$

With the same modeling method, the condenser dynamics could be represented by the following two-state model by considering the above Eq. (7):

$$A_cL_c\frac{d\rho_{\mathrm{gc}}}{dP_c}\frac{dP_c}{dt}=\dot{m}_{\mathrm{comp}}-\frac{\alpha_{\mathrm{ic}}\pi D_{\mathrm{ic}}l_c(T_{\mathrm{rc}}-T_{\mathrm{wfc}})}{h_{\mathrm{lgc}}} \quad (8)$$

$$(C_pm)_{\mathrm{wfc}}\frac{dT_{\mathrm{wfc}}}{dt}=\alpha_{\mathrm{oc}}(N_{\mathrm{cond}})A_{\mathrm{oc}}(T_{\mathrm{ac}}-T_{\mathrm{wfc}})-\alpha_{\mathrm{ic}}\pi D_{\mathrm{ic}}l_c(T_{\mathrm{wfc}}-T_{\mathrm{rc}})-\alpha_{\mathrm{icsh}}\pi D_{\mathrm{ic}}(L_c-l_c)(T_{\mathrm{wfc}}-(T_{\mathrm{rc}}+T_{\mathrm{ic}})/2) \quad (9)$$

4.5 Cargo Space. The inside temperature of this cargo space is one of the control objectives, and its dynamics can be shown by

$$\frac{dT_{\mathrm{cargo}}}{dt}=\frac{\dot{Q}_{\mathrm{out}}+\dot{Q}_{\mathrm{door}}-\dot{Q}_{\mathrm{vcc}}}{(MC)_{\mathrm{air}}} \quad (10)$$

where $\dot{Q}_{\mathrm{out}}$ represents the heating load from the ambient air, $\dot{Q}_{\mathrm{door}}$ is the load due to opening the door, and $\dot{Q}_{\mathrm{vcc}}$ represents the cooling capacity produced by the A/C-R system to balance the heating load from outside [26].

5 Simulation Model and Experimental System

By integrating the cargo space model into the A/C-R system, the whole model becomes a six-state dynamic model. The inputs are compressor speed (N_{comp}), the control frequencies of the evaporator fan variable frequency drive (N_{evap}), and condenser fan variable frequency drive (N_{cond}) which are proportional to the two fan speeds. The states $[P_e, P_c, l_e, T_{\mathrm{wfe}}, T_{\mathrm{wfc}}, T_{\mathrm{cargo}}]$ include pressures of the evaporator and condenser, the two-phase section lengths, the equivalent tube wall and fins' temperatures of two heat exchangers, and the temperature of cargo space, respectively. The output is the air temperature (T_{cargo}) of the cargo space. The Simulink model is shown in Fig. 2.

The whole experimental system is shown in Fig. 3. The A/C-R system is connected with two chambers by pipes. The condenser-side chamber can set the temperature of air sent to the condenser, whereas the temperature of air in the other chamber (called cargo space) is the controlled parameter. Among the three inputs, the two fan speeds are continuously changeable, but the compressor speed can only switch between three discreet values. Pressure sensors, thermal couples, and flow meter are installed in different locations for the measurements. The data acquisition system of national instrument is employed to collect data from the thermocouples, pressure transducers, direct current power supply, and

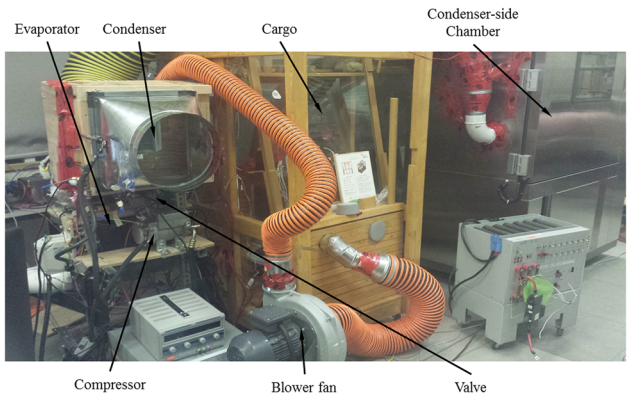

Fig. 3 Experimental system

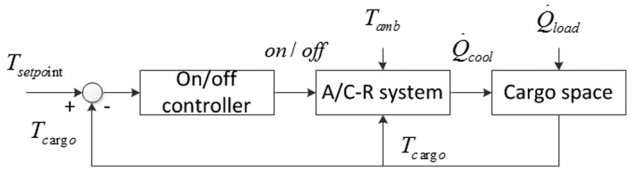

Fig. 4 Diagram of A/C-R system with on/off controller

Table 1 Operating and initial conditions

T_{amb} (°C)	T_{init} (°C)	$T_{setpoint}$ (°C)	$\dot{Q}_{out}$ (kW)	$\dot{Q}_{door}$ (kW)	N_{evap}, N_{cond} (Hz)	N_{comp} (Hz)
25	22.5	17	0.7	0.15	40	4500

flow meters, and send them to a computer. LABVIEW software is employed to obtain all the measured data from the sensors.

6 Controllers' Development

In this section, several controllers are developed and compared in terms of performance and energy consumption.

6.1 On/Off Controller. The on/off controller is most commonly used in automotive A/C-R system. Thus, the on/off controller developed in this section serves just as a basis to compare with other controllers. The on/off control strategy is actually a simple hysteresis, where the hysteresis bound is used to reduce the compressor's frequent switching [26]. The schematic of the whole system with the on/off controller is displayed in Fig. 4.

The operating conditions and initial values of some parameters are listed in Table 1.

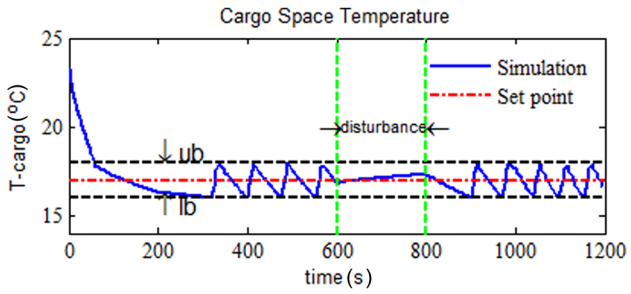

Fig. 5 Controlled temperature performance

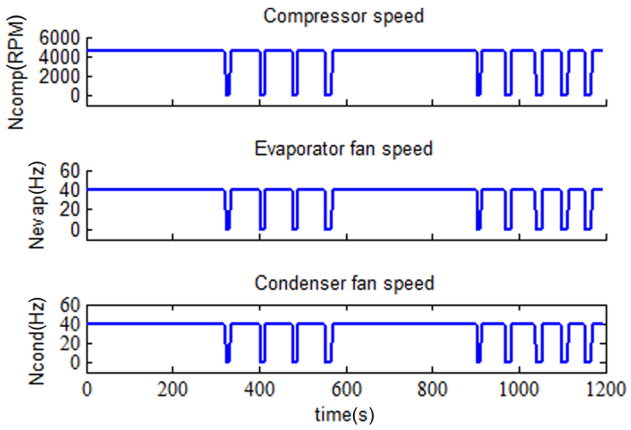

Fig. 6 Three inputs of the system

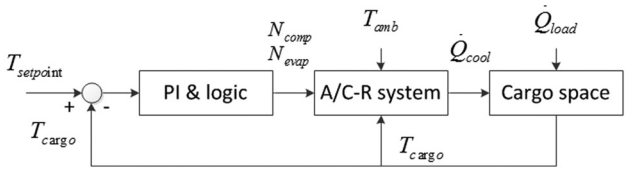

Fig. 7 Diagram of A/C-R system with PI controller

Based on the above conditions, the simulation results of the on/off controller can be obtained as shown in Figs. 5 and 6. During the 1200-s simulation, some extra heat (for 200 s) is given as a disturbance to simulate the door opening of the cargo. In Fig. 5, the temperature performance of the controller is presented. The cargo temperature could reach the set-point quickly and then fluctuate between the lower bound and the upper bound with the compressor on and off. In the extra heating load period, the compressor will be in the on mode for a longer time so that the energy consumption will be more. Figure 6 shows the system inputs during the simulation. All of them switched between the maximum speeds to zero.

6.2 Conventional PI Controller. Because of its simplicity, this controller is also commonly used in the A/C-R system with variable-speed components. Høgh and Nielsen in Ref. [7] used two separate PIs to control air temperature and superheat, respectively. In this study, the superheat is adjusted automatically by a thermostatic expansion valve such that one PI controller is utilized to manipulate evaporator fan speed. Due to the existence of a discrete input, a simple logic rule shown in Eq. (11) will be applied for compressor speed control instead of using a PI controller

$$\begin{cases} N_{comp} = 4500 & \text{if } e > 1 \\ N_{comp} = 3500 & \text{elseif } 0.5 < e \le 1 \\ N_{comp} = 2500 & \text{else} \end{cases} \tag{11}$$

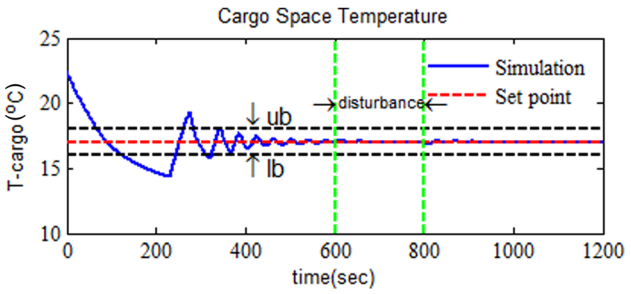

Fig. 8 Controlled temperature performance

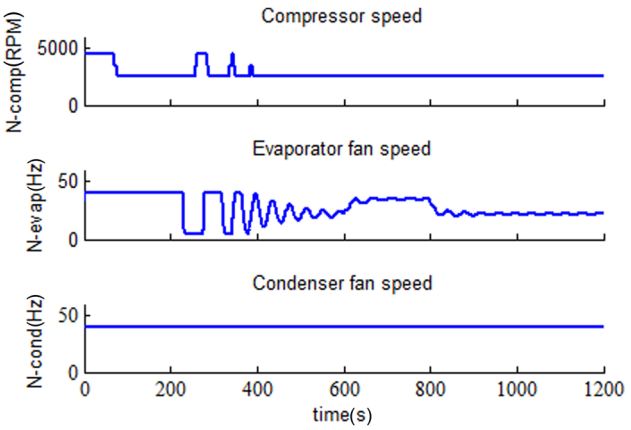

Fig. 9 Three inputs of the system

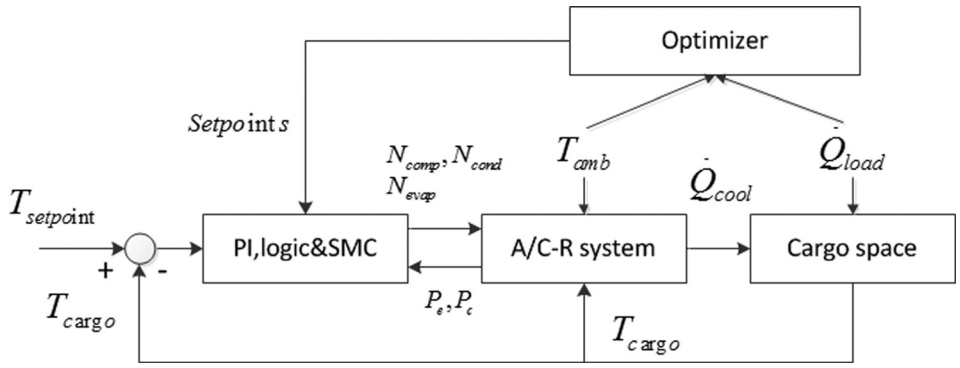

Fig. 10 Diagram of A/C-R system with set-point controller

The control system is simulated under the same operating and initial conditions shown in Table 1. The structure of the whole model is described in Fig. 7. The outputs of the controller are compressor pump speed (N_{comp}) and (N_{evap}), and they serve as two inputs for the A/C-R block; whereas, the other one input, condenser fan speed (N_{cond}), is kept unchanged at their initial values.

The temperature performance is given in Fig. 8. It can be seen that the temperature can also reach its set-point quickly but with relatively large undershoot; it takes much longer time to settle down. The gains for PI $(k_p = -0.05, k_i = -10)$ are chosen manually to improve the performance. Any further tuning did not show any improvement in the controller performance as the temperature is affected by not just compressor speed but other factors. For example, in order to stabilize the superheat, the thermostatic expansion valve will adjust its opening degree, which could change the refrigerant flow rate throughout the valve and then the air temperature. That means the high nonlinear plant cannot achieve good performance via the PI controller. Figure 9 presents the inputs of the system.

6.3 Set-Point Controller. Due to the drawbacks of the above two controllers, Larsen in Ref. [15] proposed the set-point optimizing controller by using the steady-state model of the A/C-R system.

The basic idea behind this control strategy is that the steady-state of the A/C-R system is only related to the temperature set point of the cargo space, the ambient temperature, and the heating load. That means if these parameters are kept unchanged, the A/C-R system will stay at a steady-state after settling down. However, these parameters are related to the working conditions and change in low frequency. The study of the steady-state model shows that there is a global minimum of total power consumption with respect to condenser and evaporator pressure. As a result, the condenser and evaporator pressure can be found according to the steady-state model and sent to controllers as the set-points.

In fact, the optimizer as the supervisory controller to find the set-points of two pressures according to the changes of working conditions, which is in the outer-loop and works in low frequency; whereas the inner-loop controller consists of one PI controller, one logic controller, and one SMC. The structure of this controller is shown in Fig. 10. The set-point controller could also be implemented as a lookup table to find pressure set-points based on the working condition changes. In this paper, only one working condition is considered in order to demonstrate the performance of this controller.

In the simulations below, the same initial conditions (Table 1) are used. The two pressure set-points can be found by using a gradient or other methods based on the steady-state model [15,23–25]. By using the steady-state model, the set-points are calculated: 2.55 bar for evaporator pressure and 7.8 bar for condenser pressure. Together with the air temperature set-point 17 °C, all the set-points are determined and sent to local controllers.

Table 2 Controller gains and parameters

PI controller	SMC
$k_p = -1$	$\lambda = 0.01$
$k_i = -1$	$k = 0.18,\ \phi = 0.5$

The preliminary analysis of some simulation results suggests that the condenser fan is chosen to control condenser pressure via a PI controller; whereas the evaporator fan is manipulated by a SMC to control the temperature thanks to its robustness. In this SMC, the saturation function is used instead of sign to get rid of the chattering phenomenon [30]. The sliding surface S and the control input (N_{evap}) are obtained by the sliding mode algorithm [31] and system model

$$S = \lambda(T_{\text{cargo}} - T_{\text{set-point}}) \tag{12}$$

$$N_{\text{evap}} = N_{\text{evap0}}\left\{\frac{k\text{sat}(S/\phi)\rho_{\text{air}}VC_{\text{p}_{\text{air}}} + Q_{\text{load}}}{k_{e2}A_e(T_{\text{ae}} - T_{\text{wfe}})}\right\}^{(1-k_{e1})} \tag{13}$$

The gains and the controller parameters are provided in Table 2.

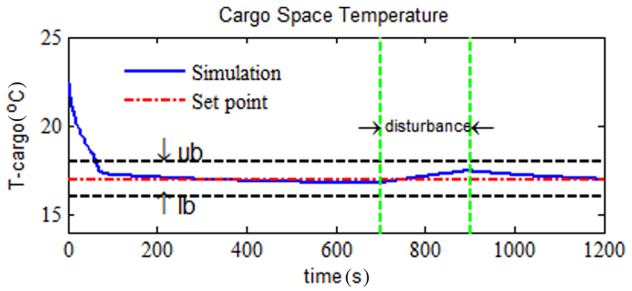

Fig. 11 Controlled temperature performance

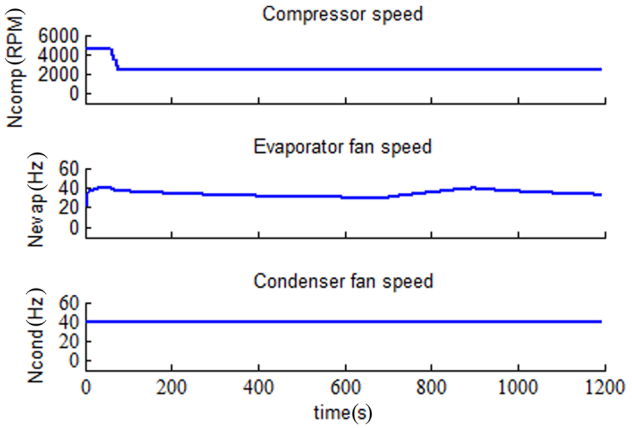

Fig. 12 Three inputs of the system

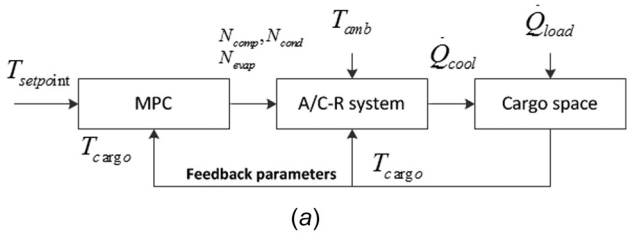

(*a*)

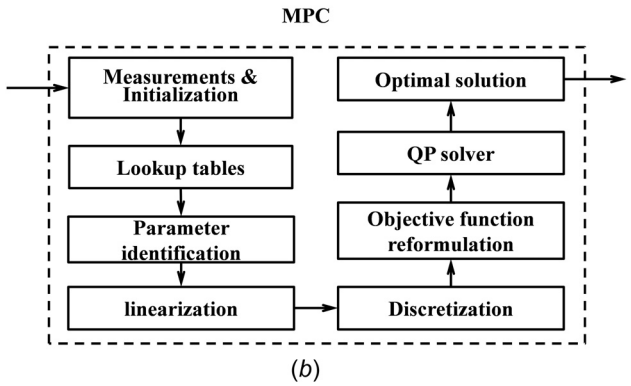

(*b*)

Fig. 13 (*a*) Diagram of A/C-R system with MPC and (*b*) structure of MPC

The cargo space temperature response is provided in Fig. 11. The temperature quickly gets to its set-point and then stays there even under the extra heating load. Figure 12 describes the three inputs of the system. Although this controller can achieve better temperature performance and fares better for energy-saving purposes; however, the controller performance is highly dependent on the working conditions. As a result, the controller's performance deteriorates as the working conditions change.

6.4 Model Predictive Controller. A linear MPC will be developed in this paper. The main idea is that an optimization problem should be solved at each time instant [32]. By introducing a prediction of horizon length and control horizon length N, the discretized objective function in next N steps will be formulated

$$J(x_0, u_0) = e(N)^{\mathrm{T}} P e(N) + \sum_{k=0}^{N-1} e(k)^{\mathrm{T}} Q e(k) + \Delta u(k)^{\mathrm{T}} S \Delta u(k)$$
$$\text{with } e(k) = y(k) - y_{\mathrm{ref}}(k), \quad k = 1, 2, \ldots N \tag{14}$$

s.t.

$$x_{\min} \le x(k) \le x_{\max}$$
$$u_{\min} \le u(k) \le u_{\max}$$
$$\Delta u_{\min} \le \Delta u(k) \le \Delta u_{\max}$$

where the first item, i.e., the final state costs, and the last item, i.e., the increment of inputs, are added in order to make the controller more robust and prevent the over-aggressive control actions. Meanwhile, the optimization problem is always subjected to some constraints. The objective function of this tracking problem is transferred into quadratic form with respect to the increment of control inputs in order to prepare to use the convex quadratic programming problem solver [32]. The convex quadratic objective function only with respect to the increment of input item is obtained by using the linearized and discretized system model and reformulating the original objective function by

$$J(x_0, u_0) = \frac{1}{2} \Delta \bar{U}^{\mathrm{T}} H \Delta \bar{U} + \Delta \bar{U}^{\mathrm{T}} g \tag{15}$$

s.t.

$$\Delta \bar{U} \ge \max(\Delta \bar{U}_{\min}(U), \ \Delta \bar{U}_{\min}(\Delta \bar{U}), \Delta \bar{U}_{\min}(X)),$$
$$\Delta \bar{U} \le \min(\Delta \bar{U}_{\max}(U), \ \Delta \bar{U}_{\max}(\Delta \bar{U}), \Delta \bar{U}_{\max}(X))$$

where the Hessian matrix (H) is symmetric and positive or semi-positive definite, and the g is the gradient vector. The constraints shown in Eq. (14) are also reformulated into the ones only related to the increment of system inputs. After solving the above problem, the first element of the optimal solution will be applied to the real system. The structure of the linear MPC is shown in Fig. 13, where the lookup tables are used to implement thermodynamic properties of the refrigerant. Then, several unknown parameters are identified and sent to the algorithm and the solver together with all other known information.

In this linear MPC, the values of controller parameters are shown in Table 3, where the time-step length (T_s) is used for

Table 3 MPC parameters

$T_s(s)$	Q	N	P	R	S
5	$100,000$	10	$1000Q$	$\begin{bmatrix} 5 & 0 & 0 \\ 0 & 0 & 0 \\ 0 & 0 & 0 \end{bmatrix}$	$\begin{bmatrix} 0 & 0 & 0 \\ 0 & 1000 & 0 \\ 0 & 0 & 1000 \end{bmatrix}$

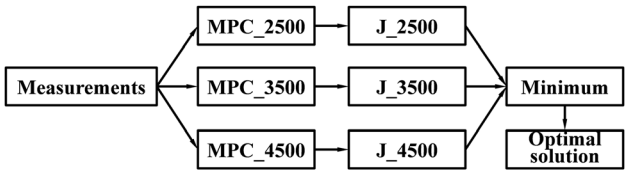

Fig. 14 Structure of the discrete MPC

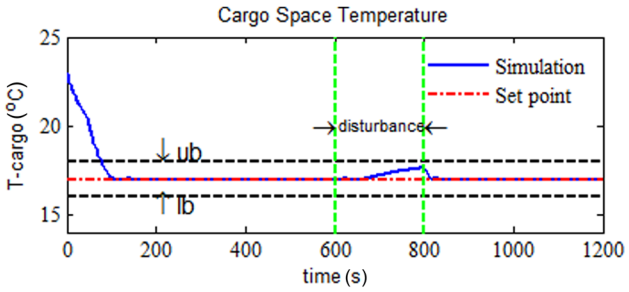

Fig. 15 Controlled temperature performance

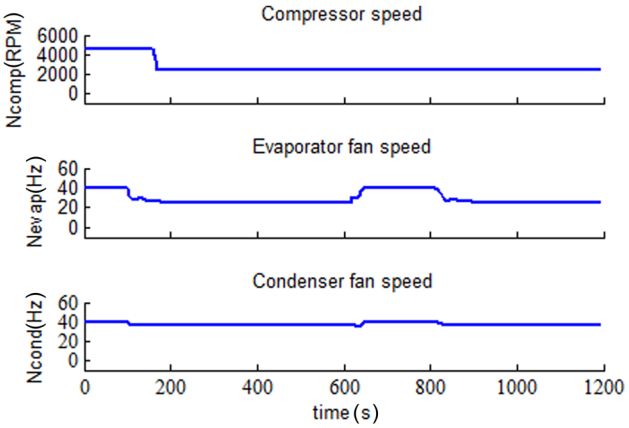

Fig. 16 Three inputs of the system

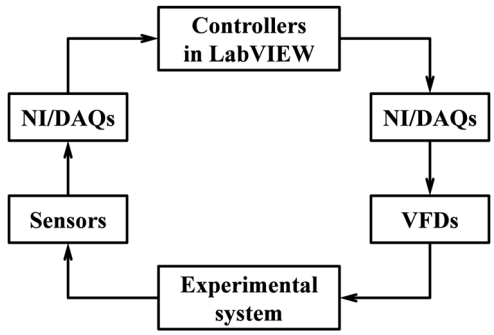

Fig. 17 Diagram of experimental system with controllers

simulation while the actual time used for one step simulation is only 0.04 s on a regular computer, which is fast enough for real-time implementation.

Because of the existence of the discrete compressor speed, a discrete MPC is developed, which is composed of three sub-MPCs as shown in Fig. 14. Three MPCs are running simultaneously at three different compressor speeds (2500, 3500, and 4500 rpm) to find the optimal solutions of other two inputs. Then, three cost values are recalculated by the two optimal input values as well as the corresponding compressor speed. By comparing their values, the minimum one will be the optimal cost of the current time instant, and the corresponding input values are the optimal solution. For example, if the J_{3500} is the minimum cost value, then the optimal solution is 3500 rpm N_{comp} as well as the optimal values of N_{evap} and N_{cond} founded by MPC_{3500}.

The simulation results are presented in Figs. 15 and 16. It can be seen from the results that the cargo temperature quickly settles down and stays there. Under the period of large disturbance brought by extra heating load, the controller tries to maintain the temperature at its set-point by increasing fan speeds of evaporator

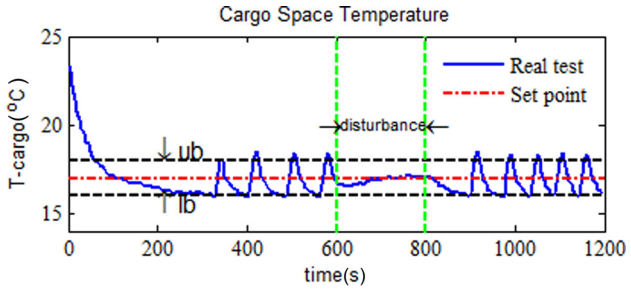

Fig. 18 Controlled temperature performance by on/off controller

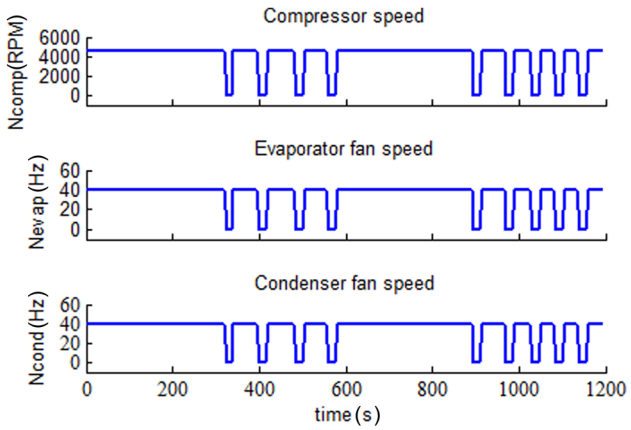

Fig. 19 Three inputs of the system by on/off controller

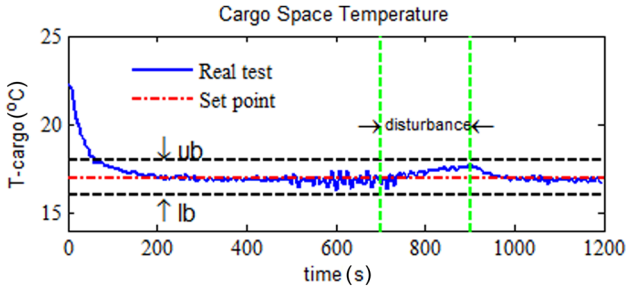

Fig. 20 Controlled temperature performance by set-point controller

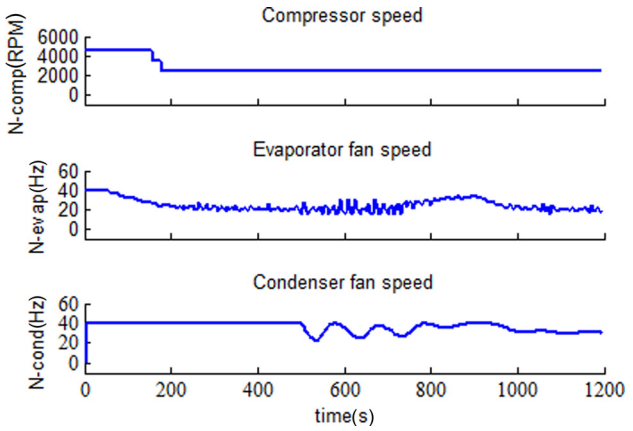

Fig. 21 Three inputs of the system by set-point controller

and condenser instead of changing the compressor speed, which is largely related to the energy consumption.

6.5 Experimental Results. The experimental system is monitored and controlled by LABVIEW software, so the first step is to implement the controllers mentioned previously. The Mathscript RT module and "Call Library Function Node" are employed for algorithm and solver implementation, respectively. The quadratic programming solver [33] originally written by c code should be converted to the dynamic link library file before the implementation. The structure of the experimental system with the embedded controllers is presented in Fig. 17.

The experimental tests are done with the controllers mentioned previously under the same working conditions as those used in simulation process. The results are shown from Figs. 18–23. It can be seen that, although the 200 s large disturbance exists, the set-point and MPC controllers can produce better control performance than that of the conventional on/off controller because of their robustness. For the sake of saving energy, the MPC penalizes the terms related to energy consumption more than that of the performance when solving the optimization problem.

Table 4 Results comparison of controllers

Controllers	On/off	PI	Set-point	MPC
MAPE between real and simulation (%)	1.92	—	1.04	1.72
MAPE between real and set-point (%)	4.20	3.03	2.18	3.00
Max APE (%)	8.9	32.15	4.28	5.91
Controller performance	Bad	Bad	Good	Good
Energy consumption (kWh-1200 s)	0.2041	0.2184	0.1818	0.1793
Energy improvement (%)	0	−5.96	9.25	10.33

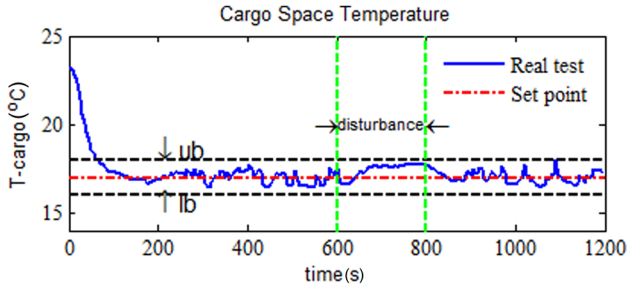

Fig. 22 Controlled temperature performance by MPC

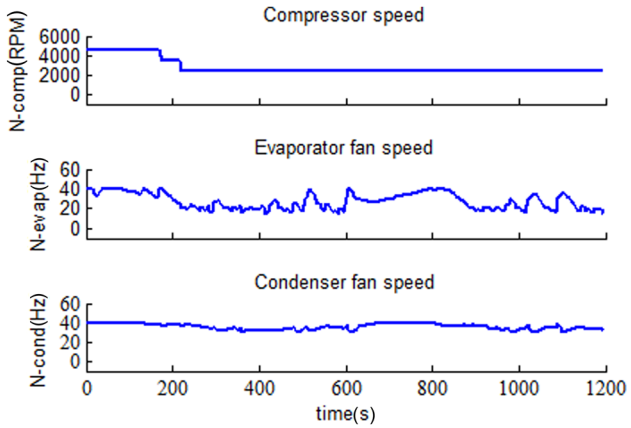

Fig. 23 Three inputs of the system by MPC

6.6 Controllers' Comparison. This section compares both experimental and simulation results obtained from each of the above controllers, and the conclusions are shown in Table 4.

Regarding the cargo space temperature performance shown in above figures, by observation, conclusions can be drawn that the on/off controller can only keep the temperature in a range; whereas the PI could reach the steady-state after experiencing a large variation from the set-point, but with bad robustness. Due to better robustness characteristics of the SMC, the set-point controller could provide a better performance. As a multivariable control strategy, the MPC is capable to deal with such complex plant. Obviously, the temperature performance of the MPC is as good as that of set-point controller not only during the dynamic period but also in the steady-state region. By data analysis, a more convinced conclusion can be drawn from the values in Table 4: both the set-point controller and MPC bring a better performance than the two conventional ones. More specifically, the first mean absolute percentage error (MAPE) measures the deviation between real and simulation temperature responses. The small MAPE values mean that the model used for the controller development has enough accuracy. The second MAPE demonstrates the offset between the temperature response and its set-point, whereas the maximum APE shows the largest drift of the temperature from its set-point. It can be seen that on/off controller and PI controller have worse performance than two others.

From the energy consumption perspective, it can be seen from Table 4 that the set-point controller and the linear MPC consume less energy than the conventional controller during the whole simulation process; this is because both of them can manipulate three inputs toward their optimal values. In order to further compare each controller, the energy consumption improvements for the controllers with respect to the on/off controller are calculated and presented in the last column of Table 4.

7 Discussion and Conclusions

This research is aimed at proposing the most energy-saving controller for automotive A/C-R systems via a comparative study on the controllers currently used by modeling, simulating, experimentally testing, and comparing each of them. Before developing the controllers, a simplified control-based model is developed and validated. Based on this model, all the controllers have been built and simulated under the same working conditions.

The comparison of simulation and experimental results shows that the set-point controller and the discrete MPC can satisfy the objectives of the A/C-R system. However, due to the high nonlinear and multi-input multi-output nature of the system, the PI controller in the set-point controller could not perform well when working conditions change fast. The discrete MPC is an optimal controller, mostly suitable for complex, multivariable, and nonlinear plants. The energy consumption term is included into the objective function when this discrete MPC is designed, which is also applicable to the real system. All of these attributes can differentiate itself from others in previous literature. Therefore, the MPC is a promising controller for A/C-R systems. Future work includes that the power consumption expression will be as a part of the objective function instead of just the quadratic form of control inputs, and the heating load from ambient environment will be identified online.

Acknowledgment

The authors would like to acknowledge the financial support of Automotive Partnership Canada (APC) and also financial and technical support of Cool-it Group.

Nomenclature

$h_{ge}(h_{gc})$ = enthalpy of vapor refrigerant
h_{ic} = enthalpy of refrigerant at the inlet of condenser
h_{ie} = enthalpy of refrigerant at the inlet of evaporator
h_{is} = isentropic of refrigerant in compressor
$h_{lc}(h_{le})$ = enthalpy of liquid refrigerant
$h_{lgc}(h_{lge})$ = latent enthalpy of refrigerant
h_{oc} = enthalpy at the outlet of condenser
j = Calburn factor
$L_c(L_e)$ = total length of the heat exchanger tube
m = total heat exchanger mass
m_{pipe} = total refrigerant mass in the pipes
$\dot{m}_v$ = refrigerant mass flow rate through the expansion valve
$\dot{m}_{comp}$ = refrigerant mass flow rate through the compressor
N_{comp} = compressor speed
N_{cond} = condenser fan control input
N_{evap} = evaporator fan control input
P_c = pressure of condenser
P_e = pressure of evaporator
Pr = Prandtl's number of air
S = slip ratio
St = Stanton number
T_a = air temperature around the heat exchanger
T_{ic} = refrigerant temperature at the inlet of condenser
$T_{rc}(T_{re})$ = saturation temperature of refrigerant
T_{sh} = superheat
$T_{wfc}(T_{wfe})$ = equivalent temperature of tube wall and fin
V_d = volumetric displacement of compressor
$\bar{\gamma}_c(\bar{\gamma}_e)$ = mean void fraction of two-phase section
η_a = adiabatic efficiency of compressor
η_{vol} = volumetric efficiency of compressor
ρ_v = density of refrigerant through the valve
$\rho_{gc}(\rho_{ge})$ = density of vapor refrigerant
$\rho_{lc}(\rho_{le})$ = density of liquid refrigerant
ρ_{ref} = density of refrigerant

References

[1] Hovgaard, T. G., Larsen, L. F. S., Edlund, K., and Jørgensen, J. B., 2012, "Model Predictive Control Technologies for Efficient and Flexible Power Consumption in Refrigeration Systems," Energy, **44**(1), pp. 105–116.

[2] Khayyam, H., Nahavandi, S., Hub, E., Kouzani, A., Chonka, A., Abawajy, J., Marano, V., and Davis, S., 2011, "Intelligent Energy Management Control of Vehicle Air Conditioning Via Look-Ahead System," Appl. Therm. Eng., **31**(16), pp. 3147–3160.
[3] Liu, J., Zhou, H., Zhou, X., Cao, Y., and Zhao, H., 2011, "Automotive Air Conditioning System Control—A Survey," 2011 International Conference on Electronic and Mechanical Engineering and Information Technology, Aug. 12–14, Harbin, Heilongjiang, China, Vol. 7, pp. 3408–3412.
[4] Leva, A., Piroddi, L., Di Felice, M., Boer, A., and Paganini, R., 2010, "Adaptive Relay-Based Control of Household Freezers With On–Off Actuators," Control Eng. Pract., **18**(1), pp. 94–102.
[5] Li, B., Otten, R., Chandan, V., Mohs, W. F., Berge, J., and Alleyne, A. G., 2010, "Optimal On–Off Control of Refrigerated Transport Systems," Control Eng. Pract., **18**(12), pp. 1406–1417.
[6] Afram, A., and Janabi-Sharifi, F., 2014, "Theory and Applications of HVAC Control Systems—A Review of Model Predictive Control (MPC)," Build. Environ., **72**, pp. 343–355.
[7] Høgh, G., and Nielsen, R., 2008, "Model Based Nonlinear Control of Refrigeration Systems," Master thesis, AAU Section for Automation and Control, Aalborg, Denmark.
[8] Petersen, A., and Lund, P. A., 2004, "Modeling and Control of Refrigeration Systems," Master thesis, Aalbory University Institute of Electronic Systems, Aalborg, Denmark.
[9] Rasmussen, B. P., and Alleyne, A. G., 2006, "Dynamic Modeling and Advanced Control of Air Conditioning and Refrigeration Systems," Air Conditioning and Refrigeration Center, College of Engineering, University of Illinois at Urbana-Champaign, Report No. TR-244.
[10] Mohanraj, M., Jayaraj, S., and Muraleedharan, C., 2012, "Applications of Artificial Neural Networks for Refrigeration, Air-Conditioning and Heat Pump Systems—A Review," Renewable Sustainable Energy Rev., **16**(2), pp. 1340–1358.
[11] Koo, B., Yoo, Y., and Won, S., 2012, "Super-Twisting Algorithm-Based Sliding Mode Controller for a Refrigeration System," 12th International Conference on Control, Automation and Systems (ICCAS), Oct. 17–21, Jeju Island, South Korea, IEEE, pp. 34–38.
[12] Shah, R., Alleyne, A. G., Bullard, C. W., Rasmussen, B. P., and Hrnjak, P. S., 2003, "Dynamic Modeling and Control of Single and Multi-Evaporator Subcritical Vapor Compression Systems," component of ACRC Project No. 123, Air Conditioning and Refrigeration Center, College of Engineering, University of Illinois at Urbana-Champaign, Urbana, IL.
[13] Rasmussen, B. P., and Alleyne, A. G., 2004, "Control-Oriented Modeling of Transcritical Vapor Compression Systems," ASME J. Dyn. Sys., Meas., Control **126**(1), pp. 54–64.
[14] He, X. D., 1996, "Dynamic Modeling and Multivariable Control of Vapor Compression Cycles in Air Conditioning Systems," Doctoral dissertation, Massachusetts Institute of Technology, Cambridge, MA.
[15] Larsen, L. F. S., 2006, "Model Based Control of Refrigeration Systems," Ph.D. dissertation, Department of Control Engineering, Aalborg University, Aalborg, Denmark.
[16] He, M., Cai, W., and Li, S., 2005, "Multiple Fuzzy Model-Based Temperature Predictive Control for HVAC Systems," Inf. Sci., **169**(1–2), pp. 155–174.
[17] Serrao, L., Onori, S., and Rizzoni, G., 2011, "A Comparative Analysis of Energy Management Strategies for Hybrid Electric Vehicles," ASME J. Dyn. Syst., Meas., Control, **133**(3), p. 031012.
[18] Ji, J., Khajepour, A., Melek, W., and Huang, Y., 2016, "Path Planning and Tracking for Vehicle Collision Avoidance Based on Model Predictive Control With Multi-Constraints," IEEE Transactions on Vehicular Technology, p. 1.
[19] Saleh, B., and Aly, A. A., 2015, "Flow Control Methods in Refrigeration Systems: A Review," Int. J. Control, Autom. Syst., **4**(1), pp. 14–23.
[20] Sørensen, K. K., Stoustrup, J., and Bak, T., 2015, "Adaptive MPC for a Reefer Container," Control Eng. Pract., **44**, pp. 55–64.
[21] Ng, B. C., Darus, I. Z. M., Jamaluddin, H., and Kamar, H. M., 2014, "Application of Adaptive Neural Predictive Control for an Automotive Air Conditioning System," Appl. Therm. Eng., **73**(1), pp. 1244–1254.
[22] Huang, G., and Dexter, A. L., 2008, "Realization of Robust Nonlinear Model Predictive Control by Offline Optimisation," J. Process Control, **18**(5), pp. 431–438.
[23] Sousa, J. M., Babuška, R., and Verbruggen, H. B., 1997, "Fuzzy Predictive Control applied to an Air-Conditioning System," Control Eng. Pract., **5**(10), pp. 1395–1406.
[24] He, X.-D., Liu, S., and Asada, H. H., 1997, "Modeling of Vapor Compression Cycles for Multivariable Feedback Control of HVAC Systems," ASME J. Dyn. Syst., Meas., Control, **119**(2), pp. 183–191.
[25] Huang, Y., Khajepour, A., Bagheri, F., and Bahrami, M., 2016, "Modelling and Optimal Energy-Saving Control of Automotive Air-Conditioning and Refrigeration Systems," Proc. Inst. Mech. Eng., Part D, epub.
[26] Li, B., 2009, "Dynamic Modeling and Control of Vapor Compression Cycle Systems With Shut-Down and Start-Up Operations," MS thesis, University of Illinois, Urbana, IL.
[27] Larsen, L. F. S., Thybo, C., Stoustrup, J., and Rasmussen, H., 2004, "A Method for Online Steady State Energy Minimization, With Application to Refrigeration Systems," 43rd IEEE Conference on Decision and Control, Dec. 14–17, Paradise Island, The Bahamas IEEE, Vol. 5, pp. 4708–4713.
[28] Larsen, L. S., Thybo, C., Stoustrup, J., and Rasmussen, H., 2003, "Control Methods Utilizing Energy Optimizing Schemes in Refrigeration Systems," European Control Conference Sept. 1–4, Cambridge, UK. IEEE, pp. 1973–1977.
[29] Larsen, L. S., and Thybo, C., 2004, "Potential Energy Savings in Refrigeration Systems Using Optimal Set-Points," Proceedings of the IEEE International Conference on Control Applications, IEEE, Vol. 1, pp. 701–704.
[30] Glaoui, H., Hazzab, A., Boussemaha, B., and Bousserhane, I. K., 2011, "SISO and MIMO Sliding Mode Control for Web Winding System," Int. Electr. Eng. J. (IEEJ), **2**(3), pp. 581–588.
[31] Benamor, A., Chrifi-alaui, L., Messaoud, H., and Chaabane, M., 2011, "Sliding Mode Control, With Integrator, for a Class of Mimo Nonlinear Systems," Engineering, **3**(5), pp. 435–444.
[32] Bemporad, A., Borrelli, F., and Morari, M., 2002, "Model Predictive Control Based on Linear Programming–The Explicit Solution," IEEE Transactions on Automatic Control, **47**(12), pp. 1974–1985.
[33] Ferreau, H. J., Kirches, C., Potschka, A., Bock, H. G., and Diehl, M., 2013, "qpOASES: A Parametric Active-Set Algorithm for Quadratic Programming," Math. Prog. Comp., **6**(4), pp. 327–363.